Materials Characterization 111 (2016) 53–59

Contents lists available at ScienceDirect

Materials Characterization

journal homepage: www.elsevier.com/locate/matchar

Microstructure and hydrogenation properties of a melt-spun non-stoichiometric Zr-based Laves phase alloy

Tiebang Zhang *, Yunlong Zhang, Jinshan Li, Hongchao Kou, Rui Hu, Xiangyi Xue

State Key Laboratory of Solidification Processing, Northwestern Polytechnical University, Xi'an 710072, China

ARTICLE INFO

Article history:
Received 27 July 2015
Received in revised form 11 November 2015
Accepted 12 November 2015
Available online 14 November 2015

Keywords:
Microstructure
Non-stoichiometric
Melt-spun
Rapid solidification
Hydrogenation properties

ABSTRACT

Alloy with composition of $Zr_{0.9}Ti_{0.1}V_{1.7}$ off normal stoichiometric proportion is selected to investigate the effect of defects introduced by non-stoichiometry on hydrogenation kinetics of Zr–Ti–V Laves phase alloys. Microstructure and phase constituent of melt-spun ribbons have been investigated in this work. The activation process, hydrogenation kinetics, thermodynamics characteristics and hydride phase constituent of as-cast alloy and melt-spun ribbons are also compared. Comparing with the as-cast alloy, the dominant Laves phase ZrV_2 is preserved, V-BCC phase is reduced and α-Zr phase is replaced by a small amount of Zr_3V_3O phase in melt-spun ribbons. Melt-spun ribbons exhibit easy activation and fast initial hydrogen absorption on account of the increased specific surface area. However, the decrease in unit cell volume of the dominant phase leads to the decrease in hydrogen absorption capacity. Melt-spinning technique raises the equilibrium pressure and decreases the stability of hydride due to the decrease of unit cell volume and the elimination of α-Zr phase, respectively. Melt-spun ribbons with fine grains show improved hydrogen absorption kinetics comparing with that of the as-cast alloy. Meanwhile, the prevalent micro twins observed within melt-spun ribbons are believed to account for the improved hydrogen absorption kinetics.

1. Introduction

Hydrogen storage is a vital part for establishing and developing a hydrogen economy society which has received considerable attention during past decades [1]. Recent research achievements and applications of hydrogen absorption materials have been summarized in recent published literatures [2–4]. Zr-based AB_2 Laves phase compounds in which B is at least one of transition metals (V, Cr, Mn, Fe, Co, Ni) have been extensively studied for their large hydrogen storage capacity, relatively easy activation, fast kinetics and long electrochemical cycle life, which can be used in the fields of metal hydride battery, non-evaporable getters, storage and separation of hydrogen and its isotopes [5–7]. ZrV_2 alloy preserves large hydrogen absorption capacity and ultralow equilibrium pressure at room temperature, but poor hydrogen absorption kinetics and large hydrogen desorption hysteresis [8–10]. Ti-doped Zr–Ti–V series alloys have been proven to be able to improve the hydrogenation properties comparing with those of the binary ZrV_2 [8,11].

Grain refinement by rapid quenching or cold rolling is an advisable way to improve hydrogenation properties of hydrogen storage alloys. Melt-spinning technique has been widely used in hydrogen storage alloys to obtain nanocrystalline, icosahedral quasicrystalline or amorphous phase. It has been proven melt-spinning technique is an efficient way to improve hydrogenation/dehydrogenation kinetics and electrochemical hydrogen storage capacities and reduce hydrogen desorption temperature of Mg-based, Ti–V-based and Ti–Zr–Ni-based alloys [12–16]. The research about $Ti_{45}Zr_{38}Ni_{17}$ ribbons in different quenching rates shows that the hydrogen storage capacity increases for the ribbons produced at high quenching rate (~45 to 50 m/s wheel speed) due to the decrease in grain size [17]. Nanocrystalline Zr–Ni–V alloys prepared by melt-spinning exhibit improved hydrogen absorption capacity and hydrogenation/dehydrogenation kinetic. Their hydrogen absorbency is comparable or even higher than the as-cast alloys with equilibrium crystalline phases [18]. Meanwhile, it has been proven melt-spinning technique can improve electrochemical hydrogen storage properties of Zr-based AB_2 alloys [19,20].

Hydrogen storage properties of alloys are always determined by the corresponding microstructural characteristics, including minor phase distribution, grain size and interface characteristics, which originate from the chemical constitute, preparing method or heat treatment history [21,22]. With a specific composition, microstructure characteristics are always determined by solidification process of different preparing methods. Understanding about the structure-activity relationship is necessary to improve hydrogenation properties of Zr-based AB_2 alloys by controlling microstructure. The effect of non-stoichiometry on hydrogenation properties of annealed $Zr_{0.9}Ti_{0.1}V_x$ ($x = 1.7$–2.3) alloys has been investigated in previous work, in which $Zr_{0.9}Ti_{0.1}V_{1.7}$ exhibits the best hydrogen absorption kinetics and capacity [23]. In the current work, it is attempted to illustrate the effect of rapidly quenched

* Corresponding author.
E-mail address: tiebangzhang@nwpu.edu.cn (T. Zhang).

http://dx.doi.org/10.1016/j.matchar.2015.11.011
1044-5803/

solidification on the microstructure and hydrogenation properties of a non-stoichiometric $Zr_{0.9}Ti_{0.1}V_{1.7}$ alloy. Microstructure and phase constituent of melt-spun ribbons are paid special attention to reveal the determining factors about hydrogenation properties of the experimental alloy. The activation process, hydrogenation kinetics, and thermodynamics parameters calculated by Van't Hoff equation of the as-cast alloy and melt-spun ribbons are compared. Meanwhile, the relationship between microstructure and hydrogen storage properties of melt-spun ribbons is proposed.

2. Experimental details

The $Zr_{0.9}Ti_{0.1}V_{1.7}$ alloy was melted in non-consumable arc melting furnace in a water-cooled copper crucible under the protection of argon atmosphere. Titanium sponge, zirconium sponge and electrolytic vanadium with purity of 99.8%, 99.4% and 99.5%, respectively, were used as raw materials. The ingot was turned over and re-melted 3 times to ensure the homogeneity. Then the ingot was re-melted in a quartz tube by induction heating and spun on a rotating single roller under an argon atmosphere of 500 mbar. The linear velocity of the casting wheel was 40 m/s. The melt-spun ribbons were obtained with a dimension of about 50 μm in thickness, 5 mm in width and 10 ~ 30 mm in length. The phase constituent of the alloy was determined by a DX-2700 powder X-ray diffractometer using Cu K_α radiation. With a step scanning mode (step width 0.03°, counting time3 seconds), the diffraction data were collected at room temperature between 20° and 80° (2θ). The microstructure of each sample was investigated by a scanning electron microscope using secondary electron imaging and a transmission electron microscope. The element distribution was determined by the Oxford INCA PentaFET × 3 EDS analyzer. Hydrogen storage properties were evaluated by a Sievert type apparatus in temperature range of 673–823 K. Prior to the absorption runs, each sample was activated by heating the sample chamber to 723 K and pumping the chamber for 30–40 min to the set vacuum in order to create a clean surface free from surface contaminations.

3. Results and discussion

3.1. Phase constituent and microstructure

The Rietveld refinement of powder X-ray diffraction pattern for melt-spun $Zr_{0.9}Ti_{0.1}V_{1.7}$ ribbons is shown in Fig. 1. The main diffraction peaks can be indexed from the diffraction angles, revealing the presence of C15-type ZrV_2, V-BCC and Zr_3V_3O phases. Previous work has shown the as-cast $Zr_{0.9}Ti_{0.1}V_{1.7}$ preserves multiphase structure with C15 ZrV_2 Laves phase, V-BCC and α-Zr phase [23]. The nonequilibrium α-Zr phase in the as-cast alloy can be eliminated and the content of V-BCC phase can be reduced by annealing treatment. Meanwhile, a small amount of Zr_3V_3O phase can be observed in the annealed alloy [23].

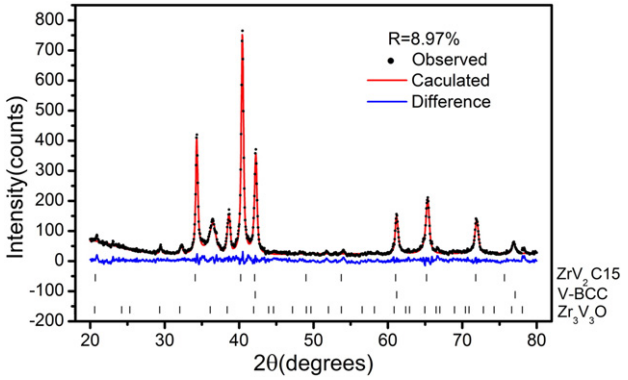

Fig. 1. Rietveld refinement of the XRD pattern for melt-spun $Zr_{0.9}Ti_{0.1}V_{1.7}$ ribbons.

The formation of Zr_3V_3O phase is probably caused by the partial oxidation of Zr and Ti sponge raw materials, oxidation during the smelting process, the long period of annealing treatment or the re-melting period of melt-spinning process. The similar results have also been observed by authors in Refs [21,24,25]. The phase content and unit cell volume of melt-spun $Zr_{0.9}Ti_{0.1}V_{1.7}$ ribbons are calculated by using the Rietveld method. The weight percent of ZrV_2, V and Zr_3V_3O in melt-spun ribbons is ~67%, ~23% and ~10% from quantitative phase analysis, respectively. The content of the dominant hydrogen absorption phase ZrV_2 increases, while the unit cell volume decreases in melt-spun alloy (0.412 nm^3) comparing with that of the as-cast one (0.415 nm^3). It is known that hydrogen atoms permeated into the bulk of alloy and stayed in the interstitial position account for the formation of hydrides. The contraction of unit cell volume can be expect to decrease in hydrogen storage capacity and increase in hydrogenation plateau pressure [26–28].

Fig. 2 shows SEM images of melt-spun $Zr_{0.9}Ti_{0.1}V_{1.7}$ ribbons. The microstructure is homogenous which mainly shows fine dendrites combined with near ZrV_2 liquid rapid solidified structure as shown in Fig. 2(a). It can be seen from Fig. 2(b) that the composition of dendritic structure is V-rich solid solutions and the size of the first dendrite is about 3–8 μm in length and 0.5 μm in width. The average secondary dendrite arm spacing is around 0.4 μm. During melt-spinning process, the liquid phase crystallizes in dendritic V-rich solid solution and ZrV_2 phase within a very short time. Comparing with the thick dendritic structure in as-cast alloy [23], the rapid quenching can restrict the growth of dendrites, refine grain and increase the number of grain

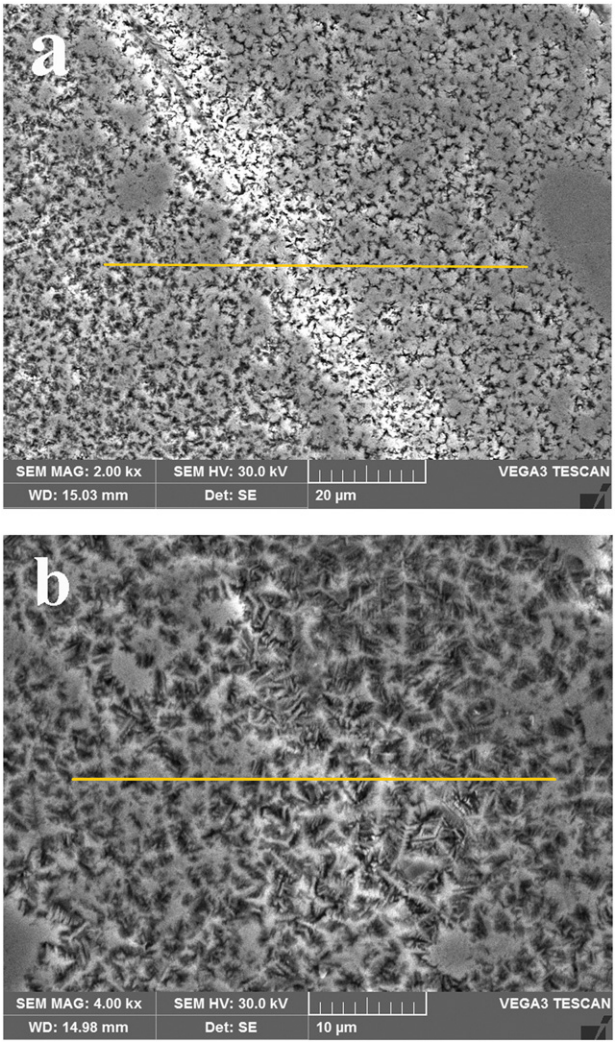

Fig. 2. SEM photographs of the melt-spun $Zr_{0.9}Ti_{0.1}V_{1.7}$ ribbons (a) 2000×, (b) 4000×.